ACS Catalysis

Research Article

pubs.acs.org/acscatalysis

Ozone-Activated Nanoporous Gold: A Stable and Storable Material for Catalytic Oxidation

Michelle L. Personick,[†] Branko Zugic,[†] Monika M. Biener,[§] Juergen Biener,[§] Robert J. Madix,[‡] and Cynthia M. Friend*[,†,‡]

[†]Department of Chemistry and Chemical Biology, [‡]School of Engineering and Applied Sciences, Harvard University, Cambridge, Massachusetts 02138, United States

[§]Nanoscale Synthesis and Characterization Laboratory, Lawrence Livermore National Laboratory, Livermore, California 94550, United States

Supporting Information

ABSTRACT: We report a new method for facile and reproducible activation of nanoporous gold (npAu) materials of different forms for the catalytic selective partial oxidation of alcohols under ambient pressure, steady flow conditions. This method, based on the surface cleaning of npAu ingots with ozone to remove carbon documented in ultrahigh vacuum conditions, produces active npAu catalysts from ingots, foils, and shells by flowing an ozone/dioxygen mixture over the catalyst at 150 °C, followed by a temperature ramp from 50 to 150 °C in a flowing stream of 10% methanol and 20% oxygen. With this treatment, all three materials (ingots, foils, and shells) can be reproducibly activated, despite potential carbonaceous poisons resulting from their synthesis, and are highly active for the selective oxidation of primary alcohols over prolonged periods of time. The npAu materials activated in this manner exhibit catalytic behavior substantially different from those activated under different conditions previously reported. Once activated in this manner, they can be stored and easily reactivated by flow of reactant gases at 150 °C for a few hours. They possess improved selectivity for the coupling of higher alcohols, such as 1-butanol, and are not active for carbon monoxide oxidation. This ozone-treated npAu is a functionally new catalytic material.

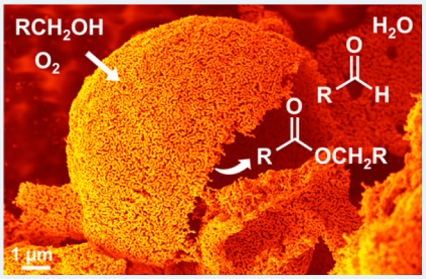

KEYWORDS: *nanoporous gold, energy-efficient catalysis, selective oxidation, activation, ozone*

INTRODUCTION

There is widespread interest in developing new catalytic materials for large-scale chemical transformations, such as selective oxidation processes, to meet the global challenge of reducing energy use. The overall objective is to design materials that continuously function as catalysts at moderate operating temperature and that have high reaction selectivity for desired products. A major objective in catalysis science is to create materials that can be reproducibly prepared and that have catalytic activity and selectivity sustained over time.

Although considerable advances have been made in the synthesis of exotic nanomaterials with tailored shapes, sizes, and compositions,[1,2] there is an ongoing need to determine how to reproducibly control their catalytic behavior and enhance their longevity. Materials that blend metal compositions and bridge multiple length scales open up a wealth of opportunities to design more energy-efficient catalysts that also maximize the economical use of resources such as precious metals.[3] However, new materials raise fresh challenges, especially in activating these materials for catalytic process and maintaining their activity and selectivity.[4]

Nanoscale Au supported on metal oxides has been widely investigated as a catalyst material for selective oxidation because the relative inertness of the gold can render high selectivity.[5−8] One important factor impeding the use of supported nanoscale gold catalysts is their propensity to agglomerate and to rapidly lose activity.[9−11] Recently, nanoporous metal materials have been prepared using a wide variety of methods, including dealloying of bulk alloys as well as bottom-up synthetic approaches.[12−23] In particular, free-standing nanoporous Au (npAu) etched from bulk Ag−Au alloys via a method that results in a dilute Ag−Au alloy (∼1−3% Ag) has been investigated as a catalyst for oxidative processes, including the selective partial oxidation of alcohols.[5,7,19,20] Nanoporous Au sustains activity over a relatively extended period,[19,20] most likely due to the nanoporous morphology, which does not readily agglomerate at moderate temperatures. The 1−3% Ag that remains in the material after this particular etching procedure is key to the activity of npAu for oxidative catalysis. The residual Ag dissociates molecular oxygen (O_2) to form adsorbed O, and the amount of Ag regulates the oxidative strength of the material.[5,18,20,24,25]

Two major challenges for the use of these nanoporous materials for catalysis are (1) activating them readily and (2)

Received: February 15, 2015
Revised: May 24, 2015
Published: May 28, 2015

DOI: 10.1021/acscatal.5b00330
ACS Catal. 2015, 5, 4237−4241

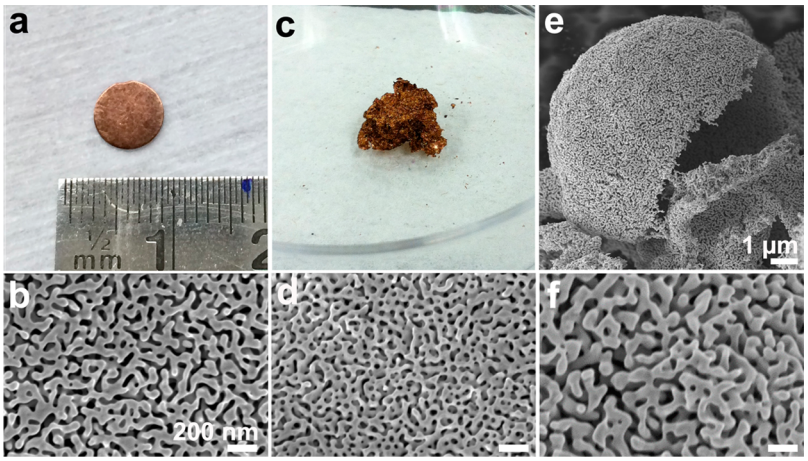

Figure 1. Photographs (a,c) and scanning electron microscopy (SEM) images (b,d-f) of freshly prepared nanoporous Au (npAu) materials used in this work: ingots (a,b), foils (c,d), and hollow shells (e,f). Images in the bottom row (b,d,f) are higher magnification SEM images of the materials in the top row (a,c,e). All scale bars in b,d,f are the same size.

sustaining their activity. The current method for activating npAu materials for catalytic partial oxidation involves flowing a mixture of reactant gases, such as CO and O_2, over the catalyst at ~75 °C until the material becomes active for CO oxidation.[19,20] Although previous work has reported successful activation of npAu catalysts using this method,[5,7,19,20] our experience is that this activation procedure is highly inconsistent and irreproducible.[26] For example, some ingots of npAu activate easily, whereas others do not activate at all, even if kept under a steady flow of reactants for many days. This variability points to a strong influence of npAu material preparation on the consistency of this approach. In addition, npAu materials that have been activated for methanol self-coupling using this method deactivate for that same reaction after exposure to higher alcohols, such as ethanol and 1-butanol. It is of key importance to develop a reliable procedure for reproducibly activating npAu materials, regardless of their method of preparation.

We have recently shown that it is necessary to remove adventitious carbon from npAu ingots to effect alcohol self-coupling reactions on npAu ingots under ultrahigh vacuum (UHV) conditions.[26] Cycles of ozone doses to the npAu surface followed by heating to approximately 600 K burn off carbon and yield ingots active for the dissociation of O_2.[26,27] However, the high annealing temperature used in these experiments results in coarsening of the npAu ingots and some accumulation of Ag at the surface. The principles developed from these studies suggest a protocol for using ozone treatment to reproducibly activate npAu materials at atmospheric pressure (including materials that cannot be activated by the previously published procedure) for catalytic oxidation. This procedure activates not only npAu ingots but also hollow npAu shells and thin npAu foils, even though the latter materials are particularly challenging to activate as a consequence of carbon incorporation resulting from their method of preparation; they could not be activated for alcohol oxidation using previously published procedures. Comparison of the catalytic behavior of ozone-activated materials with those derived from the previously published procedure suggests that these ozone-activated npAu materials are a functionally different catalytic material.

EXPERIMENTAL SECTION

Ingots of npAu were prepared via chemical etching of $Ag_{70}Au_{30}$ bimetallic alloy disks in concentrated nitric acid as previously reported (Figure 1a,b; see the Supporting Information for additional details).[5,12,13] These ingots have a diameter of ~5 mm and a thickness of 200−300 μm. Because of the high tortuosity of the npAu ingots and their known mass transport limitations for catalytic reactions,[25] we also generated thin (~100 nm thick) npAu foils (Figure 1c,d) by dealloying commercially available 6 karat white gold leaf[12,13] ($Ag_{85}Au_{15}$ alloy) and hollow spherical shells of nanoporous Au (Figures 1e,f and S1) by adapting a procedure for synthesizing hierarchically porous Au monoliths (Supporting Information).[28] The shells have an average diameter of ~8 μm and a shell thickness of 350−450 nm. Generally, the pore and ligament dimensions of the ingots, foils, and shells are very similar, ranging from 30 to 75 nm, but the characteristic pore depths of the foils and shells are 50 and 200 nm, respectively, compared with the half thickness of the ingots, 150 μm. Furthermore, the hollow shells have a BET surface area of 7.2 m^2/g, which significantly exceeds the surface area of the ingots (4.6 m^2/g).

On the basis of experiments in UHV,[26] we developed the following procedure for activating these npAu materials. First, the npAu ingots, foils, or shells were independently loaded into a flow reactor tube furnace in a glass reactor tube with a quartz frit (0.4 in. internal diameter), with the npAu lightly sandwiched between two pieces of deactivated glass wool. The temperature in the reactor was then ramped from 30 to 150 °C (10 °C/min) in a flow of 30 g/Nm^3 of ozone in a 50% O_2/He gas mixture (~3% ozone) at a total flow rate of 50 mL/min. The npAu materials were then held at 150 °C for 1 h under the same flow conditions. Subsequently, the reactor was cooled to 50 °C and then ramped from 50 to 150 °C at 10 °C/min in a flowing stream of 10% methanol and 20% O_2 (total flow rate of 50 mL/min in He). Any residual atomic oxygen from the ozone treatment is removed after a very short time in the methanol/O_2 reactant mixture. A small amount of CO_2 was evolved during this activation process as the catalyst became active for the oxidative coupling of methanol to yield methyl formate.

Because of their method of synthesis, the initial condition of the foils and shells could present extra challenges for their activation as catalytic materials. The precursor white gold leaf used to generate the foils is manufactured for use in craft processes and, thus, is not prepared with concern for residue (eg, carbon or sulfur) on the surface of the material. The hollow npAu shells are synthesized using polyvinylpyrrolidone as a stabilizing

DOI: 10.1021/acscatal.5b00330
ACS Catal. 2015, 5, 4237−4241

agent and necessitate the removal of the polystyrene core templates by calcination at 450 °C, both of which are likely to leave complex carbonaceous residue on the surface of the material. That these potential surface poisons are apparently removed during the activation process, facilitating O_2 dissociation and leading to high activity and selectivity, is a key advance of this method. These materials could not be activated for alcohol oxidation using a flowing stream of O_2 with methanol and/or CO, the activation procedure previously reported.[5,19,20]

RESULTS AND DISCUSSION

Reproducible activation of *all three* forms of npAu (ingots, foils, and shells) was achieved using the procedure described above (Figures 2 and S4). The specific activity and selectivity of the three types of npAu materials for oxidative catalysis was evaluated using the oxidation of methanol to methyl formate as a test reaction because the catalytic activity of npAu for this reaction is already well-characterized for monolithic npAu ingots.[5] Fresh samples of each of these materials could be activated without fail, whereas the previously reported method of activation of the ingots in CO/O_2 or methanol/O_2 mixtures (sometimes with added CO) at temperatures from 30 to 80 °C failed more often than it succeeded.[5,26,29] All three ozone-activated materials catalyzed the selective oxidative coupling of methanol to methyl formate in flowing gas composed of 10% methanol and 20% O_2 in He, with a total flow rate of 50 mL/min at 150 °C with 100% selectivity (Table 1). No other partial oxidation products were detected, including formaldehyde or formic acid (Figures S2 and S3). There is no quantifiable production of the combustion product, CO_2, except during activation (Figures 2 and S4).

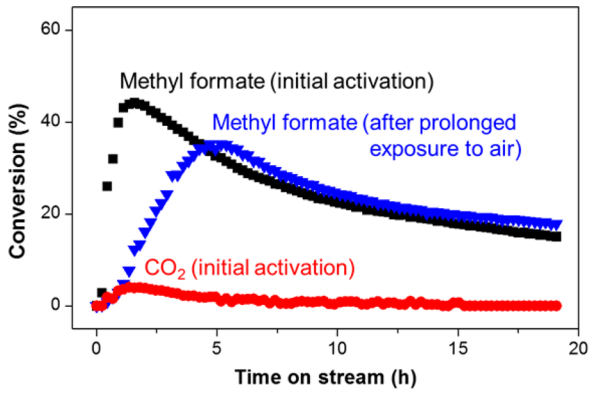

Figure 2. Conversion to methyl formate (black squares) and to CO_2 (red circles) versus time for the initial activation and stabilization period of the npAu shell catalyst in the oxidation of methanol after ozone treatment and conversion to methyl formate (blue triangles) after exposure to air for 4 months (previously activated catalyst) (~10 mg of catalyst). The temperature ramp from 50 to 150 °C takes place between the first and second time points. No carbon dioxide is produced during the reactivation after exposure to air. Similar graphs of the activation of ingots and foils are shown in Figure S4 in the Supporting Information.

Table 1. Activity of Ozone-Activated npAu Materials for the Selective Oxidation of Methanol[a]

cat. material	rate of conversion of methanol, mmol s^{-1} g^{-1}	selectivity to methyl formate, %
ingots	0.017	100
foils	0.091	100
shells	0.083	100

[a]Conditions: 10% methanol and 20% O_2 in He; flow rate, 50 mL/min; 150 °C.

These catalytic materials, activated in the manner described, show sustained and reproducible catalytic activity and selectivity. The catalysts exhibited an initial equilibration period of ~24 h, during which the activity of the catalyst increased and then gradually decreased to a stable value. This activation and stabilization period is shown in Figure 2 for ~10 mg of the npAu shell catalyst, which was well dispersed in the reactor bed and thus exhibited a high rate of methanol conversion, as reported in Table 1. Corresponding data for the ingots and foils is presented in the Supporting Information (Figure S4). The data in Figure 3, which shows sustained conversion of methanol over time, was obtained using five times the amount of the npAu shell catalyst used in Figure 2 (~50 mg) and, thus, yielded a higher conversion. The stable conversion rates of methanol for the foils and well-dispersed shells were 0.091 mmol s^{-1} g^{-1} and 0.083 mmol s^{-1} g^{-1}, respectively, which are nearly five times higher than the specific reaction rate on the ingots (0.017 mmol s^{-1} g^{-1}). The higher rates confirm that, as a result of their thinner and more open morphologies, the shells and foils do remove some of the mass transport limitations inherent to the ingots. Further, the fact that the reaction rates on the foils and shells are very similar suggests that mass transport limitations are negligible for these materials, since their characteristic pore depths differ significantly. The reaction rate on the ingots is comparable to the activity previously reported at 80 °C for ingots activated in methanol and O_2 at room temperature (0.022 mmol s^{-1} g^{-1}).[5]

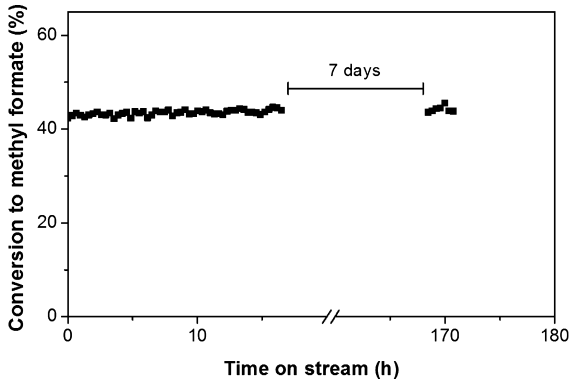

Figure 3. Steady conversion of methanol to methyl formate over the course of >7 days on activated npAu shells, after stabilization (~50 mg of catalyst). Conditions: 10% methanol and 20% O_2 in He; flow rate, 50 mL/min; 150 °C.

The initial activation of npAu creates a very robust catalyst material that can be removed from the reactor and stored in air for at least four months without losing activity. Once returned to the reactor, a few hours of exposure to the reaction conditions used for the methanol reaction (10% methanol and 20% O_2 in He, 50 mL/min, 150 °C) were required for the material to return to a stable conversion; *no reactivation in ozone was required* (Figure 2). Together, these results demonstrate the utility of this activation method for stably activating a variety of npAu catalysts, regardless of their architecture or the differences of their preparation method.

After stabilization of the catalyst following activation, no loss of catalytic activity was observed for the production of methyl formate from methanol and O_2 over an extended period of time,

DOI: 10.1021/acscatal.5b00330
ACS Catal. 2015, 5, 4237−4241

even though the surface area of the catalyst decreased as a result of coarsening of the ligament structures under reaction conditions. After 1 month of use, the surface area of the npAu shells decreased by a factor of ~10: from 7.2 to 0.7 m^2/g (BET), presumably as a result of agglomeration and a change in morphology; the ligament diameter increased from 80 ± 20 to 250 ± 80 nm (SEM) (Figure 4). Over the same period, the surface area of the npAu ingots decreased from 4.6 to 2.8 m^2/g (BET).

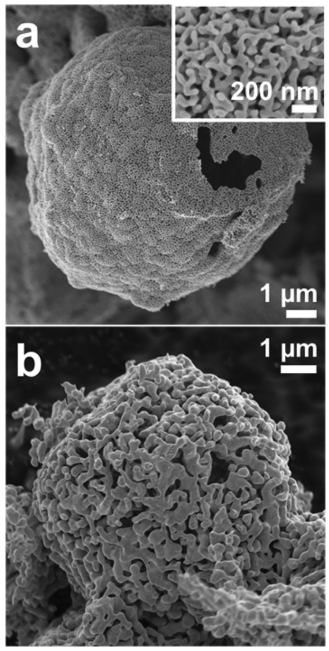

Figure 4. SEM images of the ligament sizes of the npAu shells before exposure to reactant gases (a) and after 1 month on-stream (b). Inset in a: high-magnification image of the ligament structure of the npAu shell in part a. A more detailed study of this coarsening process using the npAu foils is underway.

A minor amount of coarsening of the ligaments (from 80 ± 20 to 115 ± 25 nm) occurred on the npAu shells during the initial activation in ozone and 1−2 h under reaction conditions. After 4 days of reaction, the ligament size of the shells had increased to 140 ± 40 nm. These observations indicate that a significant amount of coarsening occurs during the early stages of reaction[30] and that the resulting rearrangement of the structure and composition of the catalyst surface may be important for the activity of the catalyst for methanol coupling in these materials. Notably, there is not a significant amount of coarsening as a result of the initial ozone treatment;[31] the coarsening occurs under reaction conditions creating the active catalyst. Studies are underway exploring the detailed relationship between coarsening and reactivity on these materials.

There are key differences between the ozone-activated npAu catalysts studied here and materials activated by simply flowing reactant mixtures over the npAu at lower temperature without ozone treatment. First, the ozone-activated npAu operates at 150 °C and above, whereas the reactant-activated ingots function (though irreproducibly) at temperatures as low as 20 °C.[5] Second, the ozone-activated catalysts show no activity for CO oxidation under standard operation conditions (no CO_2 production observed by GC/MS), whereas the other catalysts readily oxidize CO.[19,20,32,33] This difference could present an advantage for the ozone-activated materials for selective oxidation in the presence of CO.

Further, previous studies with npAu ingots activated solely with the flowing reactant stream reported only the formation of butyraldehyde from the oxidation of 1-butanol, with no evidence of the coupling product, butyl butyrate,[34] but the ozone-activated materials readily self-couple butanol. This reaction was revisited under catalytic conditions after controlled studies in UHV showed that npAu can effectively catalyze the self-coupling of 1-butanol and ethanol (see below).[35] Under a flow of 5.36% 1-butanol and 20% O_2 in He (50 mL/min), butyl butyrate was produced with selectivities of 20.6%, 11.9%, and 16.4% for the ingots, foils, and shells, respectively, with butyraldehyde as the only other reaction product (Table 2 and Figure S5).

Table 2. Rate and Selectivity for the Formation of the Self-Coupled Esters in the Selective Oxidation of and 1-Butanol on Ozone-Activated npAu Materials[a]

cat. material	ethanol self-coupling rate (selectivity[b]) mmol s^{-1} g^{-1}	1-butanol self-coupling rate (selectivity[b]) mmol s^{-1} g^{-1}
ingots	0.010 (36.1%)	0.008 (20.6%)
foils	0.014 (22.1%)	0.021 (11.9%)
shells	0.010 (20.2%)	0.016 (16.4%)

[a]Conditions: ~5% ethanol or 1-butanol and 20% O_2 in He; flow rate, 50 mL/min; 150 °C. [b]The only other product in each case is the aldehyde.

There is another important difference between the performance of the npAu catalysts activated with these two methods. On ozone-activated npAu, the selectivity to ethyl acetate in the self-coupling of ethanol (5.23% ethanol/20% O_2 in He, 50 mL/min) was stable at 36.1% for the ingots, 22.1% for the foils, and 20.2% for the shells, with the remaining product being acetaldehyde (Table 2 and Figure S6), whereas it has been reported that the self-coupling of ethanol by reactant-activated npAu shows low and variable selectivity for ethyl acetate production from day to day.[34] Both ethanol and 1-butanol self-couple at rates comparable to methanol self-coupling on the ingots (Table 1). Collectively, these observations indicate that npAu catalysts generated using the ozone activation treatment reported here are functionally different from those generated by activation in the flowing reactant stream, despite having the same general bulk composition and structure.

CONCLUSIONS

Exposure of npAu ingots, foils, or shells to a flowing stream 50% O_2/He containing ~3% ozone, followed by ramping the temperature from 50 to 150 °C in a stream of 10% methanol and 20% O_2 reproducibly activates the material for the catalytic oxygen-assisted self-coupling of primary alcohols. This procedure is effective even though the initial state of the surfaces of these different nanoporous forms varies significantly because of the methods by which they are prepared. The method is simple and reproducible. All three materials have been shown to maintain stable catalytic activity over a period of time of at least 1 week and catalyze the formation of both esters and aldehydes from ethanol and 1-butanol, which confirms the Au-like surface reactivity of these catalysts. Because of their increased accessible surface area, the npAu foils and shells generally have a higher specific rate for the production of methyl formate than do the ingots, indicating that these two morphologies mitigate the mass transport limitations inherent to npAu ingots.

DOI: 10.1021/acscatal.5b00330
ACS Catal. 2015, 5, 4237−4241

The npAu materials activated in the manner reported here show catalytic behavior functionally different from that reported in previous studies of npAu ingots activated using O_2 with methanol and/or CO.[5,19,20] The activation procedure previously reported, in which ozone was not used, activated neither the foils nor the shells and did not yield reproducible activation of the ingots for coupling reactions. The activity, selectivity, and conditions for catalytic alcohol coupling are also considerably different for the ozone-activated materials: (1) the ozone-activated npAu is inactive for CO oxidation; (2) the ozone-treated catalysts retain their activity for methanol self-coupling even when exposed to higher alcohols, unlike previous materials, which become inactive.; (3) the oxidation of 1-butanol over the new npAu catalysts leads to self-coupling to form butyl butyrate, whereas the npAu ingots activated without prior ozone treatment produced only butyraldehyde. The ozone activation has the potential to be widely applicable in activating npAu materials produced via other synthetic approaches as well as materials with other nanoporous Au alloy compositions.

■ ASSOCIATED CONTENT

Supporting Information

The Supporting Information is available free of charge on the ACS Publications website at DOI: 10.1021/acscatal.5b00330.

Additional experimental details, large area SEM image of hollow npAu shells, representative GC/MS data, and graphs of the activation of ingots and foils (PDF)

■ AUTHOR INFORMATION

Corresponding Author

*E-mail: friend@fas.harvard.edu.

Notes

The authors declare no competing financial interest.

■ ACKNOWLEDGMENTS

This work was supported as part of the Integrated Mesoscale Architectures for Sustainable Catalysis, an Energy Frontier Research Center funded by the U.S. Department of Energy, Office of Science, Basic Energy Sciences under Award No. DE-SC0012573. The microscopy work was performed at the Center for Nanoscale Systems (CNS), a member of the National Nanotechnology Infrastructure Network (NNIN), which is supported by the National Science Foundation under NSF Award No. ECS-0335765. CNS is part of Harvard University. Work at LLNL was performed under the auspices of the U.S. Department of Energy by LLNL under Contract DE-AC52-07NA27344.

■ REFERENCES

(1) Xia, Y.; Xiong, Y.; Lim, B.; Skrabalak, S. E. *Angew. Chem., Int. Ed.* **2009**, *48*, 60−103.

(2) Personick, M. L.; Mirkin, C. A. *J. Am. Chem. Soc.* **2013**, *135*, 18238−18247.

(3) Hemminger, J.; Crabtree, G.; Sarrao, J. *From Quanta to the Continuum: Opportunities for Mesoscale Science*. http://science.energy.gov/bes/news-and-resources/reports.

(4) Carrero, C. A.; Schloegl, R.; Wachs, I. E.; Schomaecker, R. *ACS Catal.* **2014**, *4*, 3357−3380.

(5) Wittstock, A.; Zielasek, V.; Biener, J.; Friend, C. M.; Bäumer, M. *Science* **2010**, *327*, 319−322.

(6) Baker, T. A.; Liu, X.; Friend, C. M. *Phys. Chem. Chem. Phys.* **2011**, *13*, 34−46.

(7) Wittstock, A.; Biener, J.; Bäumer, M. *Phys. Chem. Chem. Phys.* **2010**, *12*, 12919−12930.

(8) Haruta, M.; Kobayashi, T.; Sano, H.; Yamada, N. *Chem. Lett.* **1987**, *16*, 405−408.

(9) Kolmakov, A.; Goodman, D. W. *Catal. Lett.* **2000**, *70*, 93−97.

(10) Sykes, E. C. H.; Williams, F. J.; Tikhov, M. S.; Lambert, R. M. *J. Phys. Chem. B* **2002**, *106*, 5390−5394.

(11) Campbell, C. T.; Parker, S. C.; Starr, D. E. *Science* **2002**, *298*, 811−814.

(12) Ding, Y.; Kim, Y. J.; Erlebacher, J. *Adv. Mater.* **2004**, *16*, 1897−1900.

(13) Erlebacher, J.; Aziz, M. J.; Karma, A.; Dimitrov, N.; Sieradzki, K. *Nature* **2001**, *410*, 450−453.

(14) Chen, L. Y.; Chen, N.; Hou, Y.; Wang, Z. C.; Lv, S. H.; Fujita, T.; Jiang, J. H.; Hirata, A.; Chen, M. W. *ACS Catal.* **2013**, *3*, 1220−1230.

(15) Ma, A.; Xu, J.; Zhang, X.; Zhang, B.; Wang, D.; Xu, H. *Sci. Rep.* **2014**, *4*, 4849.

(16) Lee, M. N.; Santiago-Cordoba, M. A.; Hamilton, C. E.; Subbaiyan, N. K.; Duque, J. G.; Obrey, K. A. D. *J. Phys. Chem. Lett.* **2014**, *5*, 809−812.

(17) Déronzier, T.; Morfin, F.; Lomello, M.; Rousset, J. *J. Catal.* **2014**, *311*, 221−229.

(18) Déronzier, T.; Morfin, F.; Massin, L.; Lomello, M.; Rousset, J. *Chem. Mater.* **2011**, *23*, 5287−5289.

(19) Xu, C.; Su, J.; Xu, X.; Liu, P.; Zhao, H.; Tian, F.; Ding, Y. *J. Am. Chem. Soc.* **2007**, *129*, 42−43.

(20) Zielasek, V.; Jürgens, B.; Schulz, C.; Biener, J.; Biener, M. M.; Hamza, A. V.; Bäumer, M. *Angew. Chem., Int. Ed.* **2006**, *45*, 8241−8244.

(21) Lang, X. Y.; Guo, H.; Chen, L. Y.; Kudo, A.; Yu, J. S.; Zhang, W.; Inoue, A.; Chen, M. W. *J. Phys. Chem. C* **2010**, *114*, 2600−2603.

(22) Wang, H.; Ge, X. *Electroanalysis* **2012**, *24*, 911−916.

(23) Lee, D.; Jang, H. Y.; Hong, S.; Park, S. *J. Colloid Interface Sci.* **2012**, *388*, 74−79.

(24) Moskaleva, L. V.; Röhe, S.; Wittstock, A.; Zielasek, V.; Klüner, T.; Neyman, K. M.; Bäumer, M. *Phys. Chem. Chem. Phys.* **2011**, *13*, 4529−4539.

(25) Wittstock, A.; Neumann, B.; Schaefer, A.; Dumbuya, K.; Kübel, C.; Biener, M. M.; Zielasek, V.; Steinrück, H.; Gottfried, J. M.; Biener, J.; Hamza, A.; Bäumer, M. *J. Phys. Chem. C* **2009**, *113*, 5593−5600.

(26) Stowers, K. J.; Madix, R. J.; Friend, C. M. *J. Catal.* **2013**, *308*, 131−141.

(27) Schaefer, A.; Ragazzon, D.; Wittstock, A.; Walle, L. E.; Borg, A.; Bäumer, M.; Sandell, A. *J. Phys. Chem. C* **2012**, *116*, 4564−4571.

(28) Nyce, G. W.; Hayes, J. R.; Hamza, A. V.; Satcher, J. H. *Chem. Mater.* **2007**, *19*, 344−346.

(29) Röhe, S.; Frank, K.; Schaefer, A.; Wittstock, A.; Zielasek, V.; Rosenauer, A.; Bäumer, M. *Surf. Sci.* **2013**, *609*, 106−112.

(30) Qian, L. H.; Chen, M. W. *Appl. Phys. Lett.* **2007**, *91*, 083105.

(31) Biener, J.; Wittstock, A.; Biener, M. M.; Nowitzki, T.; Hamza, A. V.; Baeumer, M. *Langmuir* **2010**, *26*, 13736−13740.

(32) Wittstock, A.; Wichmann, A.; Biener, J.; Bäumer, M. *Faraday Discuss.* **2011**, *152*, 87−98.

(33) Fujita, T.; Tokunaga, T.; Zhang, L.; Li, D.; Chen, L.; Arai, S.; Yamamoto, Y.; Hirata, A.; Tanaka, N.; Ding, Y.; Chen, M. *Nano Lett.* **2014**, *14*, 1172−1177.

(34) Kosuda, K. M.; Wittstock, A.; Friend, C. M.; Bäumer, M. *Angew. Chem., Int. Ed.* **2012**, *51*, 1698−1701.

(35) Stowers, K. J.; Friend, C. M.; Madix, R. J.; Biener, M. M.; Biener, J. *Catal. Lett.* **2015**, *145*, 1217−1223.

DOI: 10.1021/acscatal.5b00330
ACS Catal. 2015, 5, 4237−4241